

Dynamic Stress Intensity Factors of Collinear Cracks under a Uniform Tensile Stress Wave¹

K.-C. Wu², S.-M. Huang², S.-H. Chen³

Abstract: An analysis is presented for an array of collinear cracks subject to a uniform tensile stress wave in an isotropic material. An integral equation for the problem is established by modeling the cracks as distributions of dislocations. The integral equation is solved numerically in the Laplace transform domain first and the solution is then inverted to the time domain to calculate the dynamic stress intensity factors. Numerical examples of one, two, or three collinear cracks are given. The results of one or two cracks are checked to agree closely with the existing results.

Keywords: collinear cracks, stress wave, stress intensity factor.

1 Introduction

There has been a long standing interest in the problem of plane elastic waves interacting with cracks in areas such as ultrasonic testing and dynamic fracture. The diffraction of a plane dilatational wave by a finite crack in an infinite elastic medium has been analyzed by Thau and Lu (1971) with Wiener-Hopf technique and exact but short-term stress intensity factors were obtained. It was found that the peak stress intensity factor was 30% higher than the analogous static factor. Sih and Embley (1972) considered a finite crack with normal and shear tractions applied to its surfaces using integral transforms. Itou (1980) use the same integral transform method to calculate dynamic stress intensity factors of two collinear cracks. The collinear crack configuration was also considered using boundary integral equation methods (Zhang and Achenbach, 1989; Wen, Aliabadi and Rooke, 1996). Chen and Wu (1981) developed a hybrid displacement finite element model to treat bi-material cracked structures under dynamic loadings. Various methods of modeling

¹ This paper is in honor of Professor Wen-Hwa Chen, on the occasion of his receiving the ICCES Lifetime Achievement Medal at ICCES13 in Seattle, in May 2013.

² National Taiwan University, Taipei, Taiwan.

³ National Kaohsiung University of Applied Sciences, Kaohsiung, Taiwan.

crack under static and dynamic loadings have been discussed in (Atluri, 1986). A simplified meshless method for dynamic crack growth was presented by Zhang and Chen (2008). The Symmetric Galerkin Boundary Element Method (SGBEM), and the SGBEMFEM alternating/coupling methods, were compared with the recently popularized Extended Finite Element Method (XFEM), for analyzing fracture and fatigue crack propagation in complex structural geometries by Dong and Atluri (2013a and 2013b).

One of the powerful methods for solving crack problems with static loading is the dislocation method. In this method the tractions arising along the lines of the cracks in the uncracked body are determined first. The cracks are then inserted and the unsatisfied tractions cancelled by inserting continuously varying density of dislocations, along the lines of the cracks. This formulation leads to an integral equation which may be discretized using Gaussian-Chebyshev quadrature to the desired degree of refinement (Erdogan, Gupta and Cook, 1973). The dislocation method, however, has rarely been applied to the problems concerning dynamic loading.

Cochard and Madariaga (1994) have derived an integral equation for dynamic anti-plane shear loading. The integral equation represents the traction on the crack line as the crack is considered as a distribution of dynamic dislocations. The integral equation contains a space-time convolution integral, which is Cauchy singular in space as in the static case. In addition, there is another term which is associated with radiation damping by wave emission. Recently Wu and Chen (2011) have applied the integral equation of Cochard and Madariaga (1994) to treat the problem of multiple collinear cracks subjected to normal incidence of horizontally shear wave.

In this paper the dislocation method is further extended for an array of collinear cracks under tensile stress wave. A formulation for two-dimensional elastodynamics will be introduced and used to derive the fundamental solution of a dynamic climb dislocation. The fundamental solution, in turn, will be used to construct a space-time integral equation for the problem of interest. The equation will be solved first in the Laplace transform domain using Gaussian-Chebyshev quadrature and then inverted to calculate the stress intensity factors in the time domain. Numerical examples for one, two, or three cracks of identical length will be given.

2 Formulation

For two-dimensional transient plane deformations in which the Cartesian components of the stress σ_{ij} and the displacement u_i ($i, j = 1, 2$) are independent of x_3 , the

equation of motion is

$$\mathbf{t}_{1,1} + \mathbf{t}_{2,2} = \rho \frac{\partial^2 \mathbf{u}}{\partial t^2}, \tag{1}$$

where $\mathbf{t}_1 = (\sigma_{11}, \sigma_{21})^T$, $\mathbf{t}_2 = (\sigma_{12}, \sigma_{22})^T$, \mathbf{u} is the displacement, ρ is the mass density, t is time, and a subscript comma denotes partial differentiation with respect to coordinates. The stress-strain law for isotropic materials is

$$\sigma_{ij} = \lambda \delta_{ij} u_{k,k} + \mu (u_{i,j} + u_{j,i}), \tag{2}$$

where λ and μ are Lamé constants.

For many problems such as the one considered here, the displacement depends only on $y_i = x_i/t$, $i = 1, 2$. In this case, the displacement may be expressed as (Wu, 2000)

$$\mathbf{u}(y_1, y_2) = 2Re \left[\sum_{k=1}^2 \int_{-\infty}^{w_k} f_k(w) \mathbf{a}_k(w) dw \right], \tag{3}$$

where Re stands for the real part,

$$w_k = y_1 + p_k(w_k) y_2, \tag{4}$$

$$\mathbf{a}_1(w) = (1, p_1(w))^T, \mathbf{a}_2(w) = (-p_2(w), 1)^T, \tag{5}$$

$$p_k(w) = \sqrt{\left(\frac{w}{c_k}\right)^2 - 1}, \tag{6}$$

$c_1 = \sqrt{(\lambda + 2\mu)/\rho}$ and $c_2 = \sqrt{\mu/\rho}$ are, respectively, the dilatational and shear wave speeds.

3 Integral Equation Based on Fundamental Solution for a dislocation

Consider a climb dislocation with Burgers vector $\beta = (0, \beta_2)^T$, which suddenly appears at $t = 0$. The slip plane is taken to coincide with $x_1 < 0$ and $x_2 = 0$. The continuity conditions for the traction \mathbf{t}_2 and the jump conditions for the displacement \mathbf{u} across the slip plane are given by

$$\mathbf{t}_2^+(x_1, t) - \mathbf{t}_2^-(x_1, t) = \mathbf{0}, \tag{7}$$

$$\mathbf{u}^+(x_1, t)_{,1} - \mathbf{u}^-(x_1, t)_{,1} = -\delta(x_1) H(t) \beta, \tag{8}$$

where the superscripts "+" and "-" denote the limiting values as $x_2 \rightarrow 0^+$ and $x_2 \rightarrow 0^-$, respectively, δ the Dirac delta function and H the unit step function.

For $t > 0$ substitution of Eq.3 into Eq.7 and Eq.8 leads to

$$\begin{aligned} 2\text{Re} \left[\sum_{k=1}^2 (f_k^+(y_1) - f_k^-(y_1)) \mathbf{b}_k(y_1) \right] &= 0, \\ 2\text{Re} \left[\sum_{k=1}^2 (f_k^+(y_1) - f_k^-(y_1)) \mathbf{a}_k(y_1) \right] &= -\delta(y_1) \beta, \end{aligned} \tag{9}$$

where \mathbf{b}_1 and \mathbf{b}_2 are given by

$$\mathbf{b}_1(w) = \mu (2p_1(w), p_2^2(w) - 1)^T, \mathbf{b}_2 = \mu (1 - p_2^2(w), 2p_2(w))^T. \tag{10}$$

It may be shown that for $y_2 = 0$,

$$\begin{aligned} \mathbf{a}_1^T \mathbf{b}_2 + \mathbf{b}_1^T \mathbf{a}_2 &= \mathbf{a}_1^T \bar{\mathbf{b}}_2 + \mathbf{b}_1^T \bar{\mathbf{a}}_2 = 0, \\ \mathbf{a}_1^T \bar{\mathbf{b}}_1 + \mathbf{b}_1^T \bar{\mathbf{a}}_1 &= \mathbf{a}_2^T \bar{\mathbf{b}}_2 + \mathbf{b}_2^T \bar{\mathbf{a}}_2 = 0. \end{aligned} \tag{11}$$

Eq.9 with Eq.11 yields

$$f_k^+(y_1) - f_k^-(y_1) = -\frac{\delta(y_1)}{\gamma_k(y_1)} \mathbf{b}_k^T \beta \tag{12}$$

where $\gamma_k = 2\mathbf{a}_k^T \mathbf{b}_k = 2\mu (1 + p_2^2) p_k$. The solution of $f_k(w_k)$ is readily obtained as

$$f_k(w_k) = \frac{1}{2\pi i w_k \gamma_k} \mathbf{b}_k^T(w_k) \beta, \tag{13}$$

where the following identity is utilized:

$$\lim_{\varepsilon \rightarrow 0} \frac{1}{y_1 \pm i\varepsilon} = \frac{1}{y_1} \mp \pi i \delta(y_1). \tag{14}$$

Substituting Eq.13 into Eq.3, the corresponding \mathbf{u} for $x_2 > 0$ is given by

$$\mathbf{u}(y_1, y_2) = \frac{1}{\pi} \text{Im} \left[\sum_{k=1}^2 \int_{\infty}^{w_k} \frac{1}{w \gamma_k(w)} \mathbf{a}_k \mathbf{b}_k^T dw \right] \beta, \tag{15}$$

where Im stands for the imaginary part. For $x_1 < -\sqrt{c_k^2 t^2 - x_2^2}$ and $0 < x_2 < c_k t$, Eq.15 yields

$$\mathbf{u}(y_1, y_2) = \frac{1}{2} H(c_1 - y_2) \beta. \tag{16}$$

The derivation for Eq.16 is shown in Appendix A. From Eq.2 and Eq.15, the stress vector \mathbf{t}_2 is given by

$$\mathbf{t}_2(x_1, x_2, t) = -\frac{\rho c_1}{2} \delta\left(t - \frac{x_2}{c_1}\right) H(-x_1) \beta + \frac{1}{\pi} \text{Im} \left[\sum_{k=1}^2 \frac{1}{w_k \gamma_k(w_k)} \frac{\partial w_k}{\partial x_1} \mathbf{b}_k \mathbf{b}_k^T \right] \beta.$$

(17)

where the first term on the right side corresponds to the normal plane wave moving away from the slip plane and the second term is due to the bulk wave emitted from the dislocation. As $x_2 \rightarrow 0^+$, Eq.17 yields

$$\sigma_{22}(x_1, t) = -\frac{\rho c_1}{2} \delta(t) H(-x_1) \beta_2 + \frac{1}{2\pi x_1} V_2(y_1) \beta_2, \quad (18)$$

where

$$V_2(y_1)/\mu = \left(\frac{4\sqrt{1 - (y_1/c_2)^2}}{(y_1/c_2)^2} \right) H(c_2 - y_1) - \frac{(2 - (y_1/c_2)^2)^2}{(y_1/c_2)^2 \sqrt{1 - (y_1/c_1)^2}} H(c_1 - y_1). \quad (19)$$

For a continuous distribution of dislocation density $\alpha_2(\xi_1, \tau)$, where $-\infty < \xi_1 < \infty$ and $0 < \tau < t$, the Burgers vector for the dislocation at $x_1 = \xi_1$ appearing at time τ is given by

$$d\beta_2 = \frac{\partial \alpha_2(\xi_1, \tau)}{\partial \tau} d\tau d\xi_1. \quad (20)$$

From Eq.18 the corresponding $\sigma_{22}(x_1, t)$ is

$$\sigma_{22}(x_1, t) = -\frac{\rho c_1}{2} \int_{x_1}^{\infty} \frac{\partial \alpha_2(\xi_1, t)}{\partial t} d\xi_1 + \frac{1}{2\pi} \int_{-\infty}^{\infty} \frac{1}{x_1 - \xi_1} \int_0^t V_2\left(\frac{x_1 - \xi_1}{t - \tau}\right) \frac{\partial \alpha_2(\xi_1, \tau)}{\partial \tau} d\tau d\xi_1. \quad (21)$$

Eq.21 may be used for cracks under dynamic loadings by setting the crack opening displacement Δu_2 as

$$\Delta u_2(x_1, t) = \int_{x_1}^{\infty} \alpha_2(\xi_1, t) d\xi_1. \quad (22)$$

with the stresses

$$\sigma_{22}(x_1, t) = -p(x_1, t) \quad (23)$$

applied to the crack faces, where $p(x_1, t)$ are the stresses due to applied loading in the absence of the cracks.

4 Numerical Implementation

Consider M collinear cracks located at $|x_1 - b_i| \leq a_i, i = 1, \dots, M$ and $x_2=0$ in an infinite body For $|x_1 - b_i| \leq a_i$, Eq.21 with Eq.23 gives

$$\begin{aligned}
 p(b_i + a_i x, t) &= \frac{\rho c_1 a_i}{2} \int_x^1 \frac{\partial \alpha_2(b_i + a_i \xi, t)}{\partial t} d\xi \\
 &+ \frac{1}{2\pi} \sum_{j=1}^N \int_{-1}^1 \frac{a_j}{b_j + a_j \xi - b_i - a_i x} \int_0^t V_2 \left(\frac{b_j + a_j \xi - b_i - a_i x}{t - \tau} \right) \frac{\partial \alpha_2(b_j + a_j \xi, \tau)}{\partial \tau} d\tau d\xi,
 \end{aligned}
 \tag{24}$$

where $|x| \leq 1, |\xi| \leq 1$ and the following crack closure conditions from (22) have been enforced:

$$\int_{-1}^1 \alpha_2(b_i + a_i \xi, t) d\xi = 0, \quad i = 1, 2, \dots, M.
 \tag{25}$$

Taking the Laplace integral transform in time on Eq.24 yields

$$\begin{aligned}
 \hat{p}(b_i + a_i x, s) &= \frac{\rho c_1 a_i s}{2} \int_x^1 \hat{\alpha}_2(b_i + a_i \xi, s) d\xi \\
 &+ \frac{\mu}{2\pi} \sum_{j=1}^M \int_{-1}^1 \frac{U_I(s |b_j + a_j \xi - b_i - a_i x| / c_1)}{b_j + a_j \xi - b_i - a_i x} \hat{\alpha}_2(b_j + a_j \xi, s) a_j d\xi,
 \end{aligned}
 \tag{26}$$

where

$$U_I(z) = 4(K_2(mz) - K_2(z)/m^2) + 4(1 - 1/m^2)zK_1(z) - m^2z \int_z^\infty K_0(\eta) d\eta, \tag{27}$$

$(\hat{\sigma}_{22}, \hat{\alpha}_2) = \int_0^\infty (\sigma_{22}, \alpha_2) e^{-st} dt, m = c_1/c_2 = \sqrt{2(1-\nu)/(1-2\nu)}$, ν is Poisson's ratio. In Eq.27 K_n is the modified Bessel function of order n . The derivation for Eq.27 is given in Appendix B.

It can be shown that as $x_1 \rightarrow \xi_1$, or $z \rightarrow 0, U_I(z) \rightarrow 2(1 - 1/m^2)$ so that Eq.26 is a singular integral equation of Cauchy type. To incorporate the square-root singularity of α_2 at $\xi_1 = b_j \pm a_j$, let

$$\hat{\alpha}_2(b_j + a_j \xi, s) = \frac{\hat{g}_j(\xi, s)}{a_j \sqrt{1 - \xi^2}},
 \tag{28}$$

where \hat{g}_j is finite at $\xi = \pm 1$. Substitution of Eq.28 into Eq.26 leads to (Erdogan, Gupta and Cook, 1973)

$$\begin{aligned}
 \hat{p}(b_i + a_i x, s) &= \frac{\rho c_1 s}{2} \int_x^1 \frac{\hat{g}_i(\xi, s)}{\sqrt{1 - \xi^2}} d\xi \\
 &+ \frac{\mu}{2\pi} \sum_{j=1}^M \int_{-1}^1 \frac{U_I(s |b_j + a_j \xi - b_i - a_i x| / c_1)}{b_j + a_j \xi - b_i - a_i x} \frac{\hat{g}_j(\xi, s)}{\sqrt{1 - \xi^2}} d\xi.
 \end{aligned}
 \tag{29}$$

Eq.29 can be expressed in terms of Gauss-Chebyshev quadrature of order N as

$$\hat{p}_i^{(\ell)} = \frac{\rho c_1 s}{N_c} \sum_{k=1}^N \left[\left(\sum_{m=1}^{N-1} \frac{\cos(m\varphi^{(k)}) \sin(m\theta^{(\ell)})}{m} \right) \right] \hat{g}_i^{(k)} + \frac{\mu}{2N_c} \sum_{j=1}^M \sum_{k=1}^N \frac{U_I(s|b_i + a_i x^{(\ell)} - b_j - a_j \xi^{(k)}|/c_1)}{b_j + a_j \xi^{(k)} - b_i - a_i x^{(\ell)}} \hat{g}_j^{(k)}, \quad i = 1, \dots, M \quad (30)$$

where

$$\hat{p}_i^{(\ell)} = \hat{p}(b_i + a_i x^{(\ell)}, s), \quad \hat{g}_i^{(k)} = \hat{g}_i(\xi^{(k)}, s), \quad (31)$$

$$\xi^{(k)} = \cos(\varphi^{(k)}), \quad \varphi^{(k)} = (k - 1/2)\pi/N, \quad k = 1, 2, \dots, N, \quad (32)$$

$$x^{(\ell)} = \cos(\theta^{(\ell)}), \quad \theta^{(\ell)} = \ell\pi/N, \quad \ell = 1, 2, \dots, N - 1, \quad (33)$$

Similarly Eq.25 can be expressed as

$$\sum_{k=1}^N \hat{g}_i^{(k)} = 0, \quad i = 1, \dots, M, \quad (34)$$

The derivation for Eq.30 and Eq.34 is shown in Appendix C. The unknowns $\hat{g}_i^{(k)}, i = 1, \dots, M, k = 1, 2, \dots, N$, may be solved from Eq.30 and Eq.34.

The stress intensity factors of the crack tips $x_1 = b_i \pm a_i$ in the Laplace transform domain can be obtained by

$$\hat{K}_I(b_i + a_i, s) = \frac{\mu}{1 - \nu} \frac{1}{2N} \sqrt{\frac{\pi}{a_i}} \sum_{k=1}^N (-1)^{k+1} \cot \frac{\varphi^{(k)}}{2} \hat{g}_i^{(k)}, \quad (35)$$

$$\hat{K}_I(b_i - a_i, s) = \frac{\mu}{1 - \nu} \frac{(-1)^N}{2N} \sqrt{\frac{\pi}{a_i}} \sum_{k=1}^N (-1)^{k+1} \tan \frac{\varphi^{(k)}}{2} \hat{g}_i^{(k)}, \quad (36)$$

The derivation for Eqs.35 and 36 can be found in Appendix C. The inversion of Eq.35 to the time domain is carried out using the method proposed by Durbin (1974) as

$$K_I(b_i \pm a_i, t) = \frac{e^{s_0 t}}{T} \text{Re} \{ \hat{K}_I(b_i \pm a_i, s_0) \} + \frac{2e^{s_0 t}}{T} \text{Re} \left\{ \sum_{k=1}^{N_S} \hat{K}_I(b_i \pm a_i, s_k) e^{ik2\pi t/T} \right\}, \quad (37)$$

where $s_k = s_0 + ik2\pi/T, k = 0, 1, 2, \dots, N_S, s_0$ and T are adjustable parameters.

5 Numerical Examples

In this section the proposed numerical method is applied to calculate the transient stress intensity factors for one, two, or three collinear cracks of length $2a$ under the normal incidence of a uniform tensile stress wave, $p(x_1, t) = p_0 H(t)$. The results are displayed in terms of the dimensionless stress intensity factor $K_I' = K_I / p_0 \sqrt{\pi a}$ and the dimensionless time $t' = c_1 t / a$.

5.1 One Crack

Consider a crack as shown in Fig.1. The Poisson's ratio ν is taken as 0.25. The corresponding ratios of the shear and Rayleigh wave speeds to the dilatational wave speed are, respectively, $c_2/c_1 = 0.58$ and $c_R/c_1 = 0.53$. The plot of K_I' as a function of t' is shown in Fig. 2. The analytic result given by Thau and Lu (1971) for $t' < 4$ is also plotted in Fig. 2. Close agreement of our result with that of Thau and Lu (1971) can be observed. The peak value of K_I' is 1.32, which occurs at the first kink at $t' = 3.77$ when the first Rayleigh wave from one the crack tip reaches the tip. The second kink appears at $t' = 7.54$ as the Rayleigh wave from the tip is reflected by the other tip back to the tip [Wen, Aliabadi and Rooke, 1996].

5.2 Two Collinear Cracks

Consider the two collinear cracks shown in Fig. 3. The Poisson's ratio ν is taken as 0.29. The corresponding ratios of the shear and Rayleigh wave speeds to the dilatational wave speed are, respectively, $c_2/c_1 = 0.54$ and $c_R/c_1 = 0.50$. The plots of K_I' as a function of t' for the inner tip B and outer tip A are given in Fig. 4. The numerical results reported by Itou (1980) are also plotted in Fig. 4. It is seen that our results agree closely with those of Itou (1980). The peak values of the stress intensity factors are 1.34 and 1.31 for tips B and A, respectively, which occur as the Rayleigh wave traveling from one tip reaches the other.

5.3 Three Collinear Cracks

Consider three collinear cracks shown in Fig. 5. The Poisson's ratio ν is taken as 0.29. The plots of K_I' as a function of t' for the inner tip A, B and C are shown in Fig. 6. The peak values of the stress intensity factor are 1.30, 1.34, and 1.37 for tip A, B and C, respectively. The peak values of the stress intensity factors for tip A and B occur at $t' = 3.97$ when the Rayleigh waves from crack tip B and A arrive at tip A and B, respectively. The peak value of the stress intensity factors for tip C occurs at $t' = 10.0$ when the Rayleigh wave starting from the tip at $x_1 = 4a$ arrives at tip C.

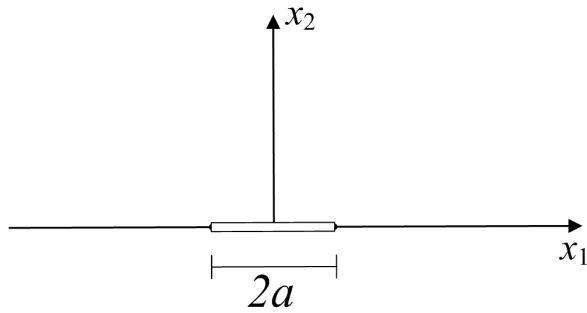


Figure 1: Configuration of a crack

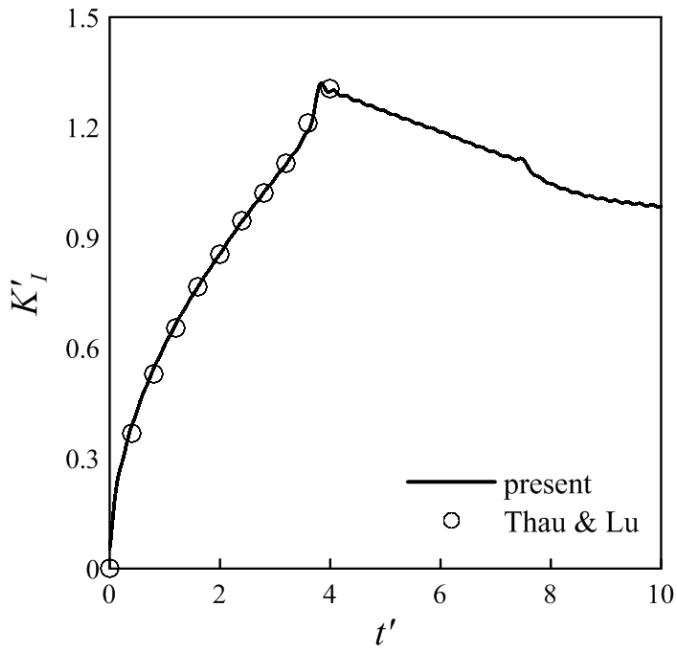


Figure 2: Stress intensity factor as a function of time for one crack

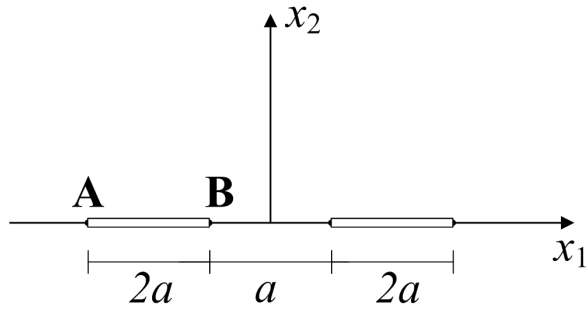


Figure 3: Configuration of two cracks

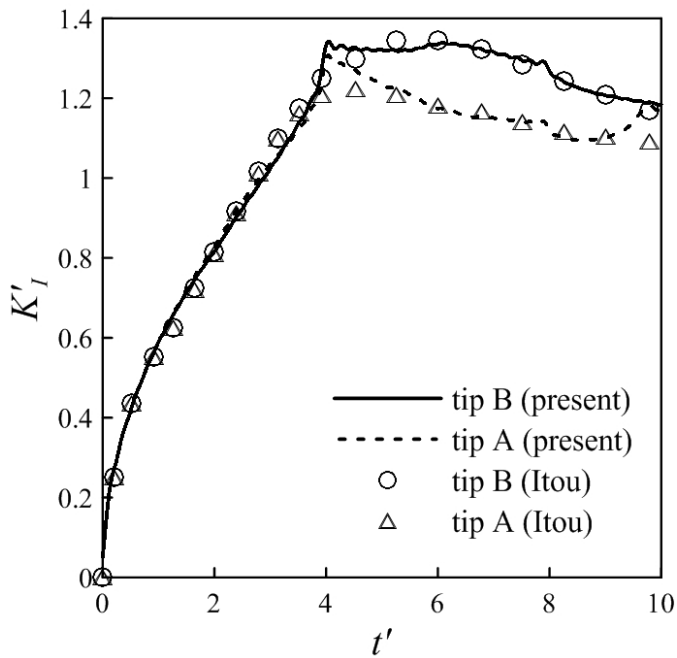


Figure 4: Stress intensity factors as a function of time for two cracks

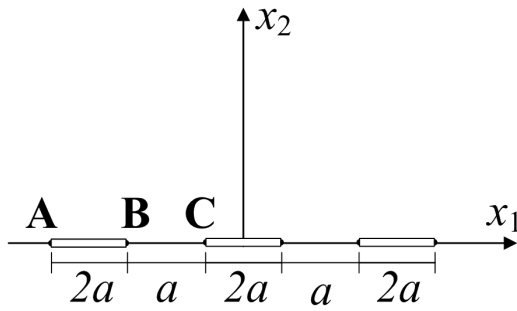


Figure 5: Configuration of three cracks

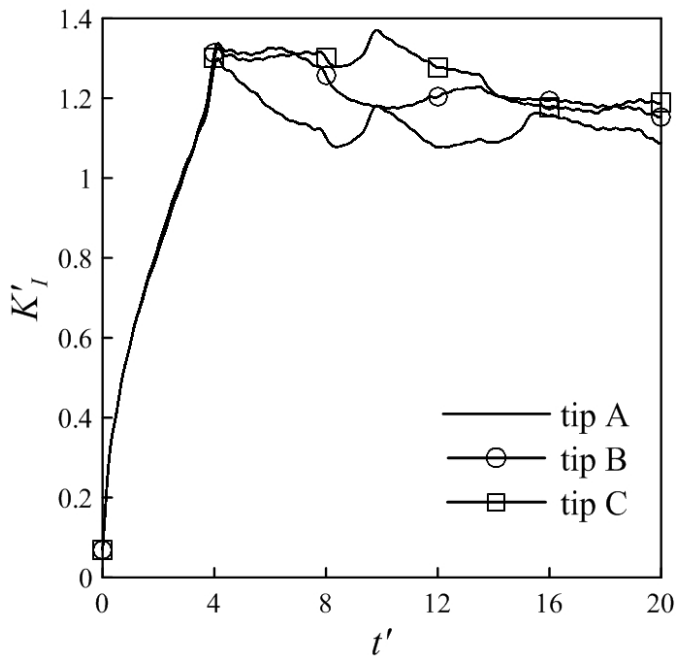


Figure 6: Stress intensity factors as a function of time for three cracks

6 Conclusions

Mode I stress intensity factors of an array of collinear cracks in isotropic solids subjected to normal incidence of uniform tensile stress waves have been studied using a dislocation method. The numerical examples for one, two or three cracks show that the present method is effective and accurate. The method can be extended to treat oblique incidence of stress waves, which result in mode II as well as Mode I stress intensity factors. The work is in progress and will be reported in a separate communication.

Acknowledgement

The research was supported by the National Science Council of Taiwan under grant NSC 101-2221-E-002-086-MY2.

References

- Atluri, S. N.** (1986): *Computational methods in the mechanics of fracture* (Vol. 2). Amsterdam: North-Holland.
- Chen, W. H.; Wu, C. W.** (1981): On elastodynamic fracture mechanics analysis of bi-material structures using finite element method. *Engineering Fracture Mechanics*, vol. 15, no. 1-2, pp. 155-168.
- Cochard, A.; Madariaga, R.** (1994): Dynamic faulting under rate-dependent friction. *Pure and Applied Geophysics*, vol. 142, no. 3/4, pp. 419-445.
- Dong, L.; Atluri, S. N.** (2013): Fracture & Fatigue Analysis: SGBEM-FEM or XFEM? Part 1: 2D structures. *CMES: Computer Modeling in Engineering & Sciences*, vol. 90, no. 2, pp. 91-146.
- Dong, L.; Atluri, S. N.** (2013): Fracture & Fatigue Analysis: SGBEM-FEM or XFEM? Part 2: 3D solids. *CMES: Computer Modeling in Engineering & Sciences*, vol. 90, no. 2, pp. 379-413.
- Durbin, F.** (1974): Numerical inversion of Laplace transforms: an efficient improvement to Dubner and Abate's method. *The computer Journal*, vol. 17, pp. 371-376.
- Erdogan, F.; Gupta, G. D.; Cook, T. S.** (1973): Numerical solution of singular integral equations. *Methods of analysis and solutions of crack problems* (edited by Sih, G. C.). Leyden: Noordhoff; pp. 368-425.
- Itou, S.** (1980): Transient analysis of stress waves around two coplanar Griffith cracks under impact load. *Engineering Fracture Mechanics*, vol. 13, pp. 349-356.
- Sih, G. C.; Embley, G. T.** (1972): Impact response of a finite crack in plane exten-

sion. *International Journal of Solids and Structures*, vol. 8, pp. 977-993.

Thau, S. A.; Lu, T. H. (1971): Transient stress intensity factors for a finite crack in an elastic solid caused by a dilatational wave. *International Journal of Solids and Structures*, vol. 7, pp. 731-750.

Wen, P. H.; Aliabadi, M. H.; Rooke, D. P. (1996): The influence of elastic waves on dynamic stress intensity factors (two-dimensional problems). *Archive of Applied Mechanics*, vol. 66, pp. 326-335.

Wu, K. C. (2000): Extension of Stroh's formalism to self-similar problems in two-dimensional elastodynamics. *Proceeding of the Royal Society of London*, A456, pp. 869-890.

Wu, K. C.; Chen, J. C. (2011): Transient analysis of collinear cracks under anti-plane dynamic loading. *Procedia Engineering*, vol. 10, pp. 924-929.

Zhang, C. H.; Achenbach, J. D. (1989): Time-domain boundary element analysis of dynamic near-tip fields for impact-loaded collinear cracks. *Engineering Fracture Mechanics*, vol. 32, no. 6, pp. 899-909.

Zhang, Y. Y.; Chen, L. (2008): A simplified meshless method for dynamic crack growth. *CMES: Computer Modeling in Engineering & Sciences*, vol. 31, no. 3, pp. 189-200.

Appendix A Derivation for Eq.16

From Eq.4 and Eq.6, the explicit expression for w_k can be obtained as

$$w_k = \frac{y_1 + y_2 \sqrt{(y/c_k)^2 - 1}}{1 - (y_2/c_k)^2} \quad (A1)$$

where $y = \sqrt{y_1^2 + y_2^2}$. From Eq. A1, the w_k -values for $x_1 < -\sqrt{c_k^2 t^2 - x_2^2}$ and $0 < x_2 < c_k t$ are real and negative. Since the integrand of Eq.A1 is real if w is real, the integration contour can be extended to $w_k \rightarrow -\infty$ without changing the value of the integral. By Cauchy's integral theorem the contour can be further replaced by a semi-circle with infinite radius in the upper w -plane, i.e., $w = Re^{i\theta}$, $R \rightarrow \infty$, $0 < \theta < \pi$. The resulting expression is

$$\mathbf{u}(\eta_1, \eta_2) = \frac{1}{\pi} \lim_{R \rightarrow \infty} \sum_{k=1}^2 \int_0^\pi \frac{1}{\gamma_k(Re^{i\theta})} \mathbf{a}_k(Re^{i\theta}) \mathbf{b}_k^T(Re^{i\theta}) d\theta \quad (A2)$$

As $R \rightarrow \infty$

$$\begin{aligned} \mathbf{a}_1 &= \frac{w}{c_1} (0, 1)^T, & \mathbf{a}_2 &= -\frac{w}{c_2} (1, 0)^T \\ \mathbf{b}_1 &= \rho w^2 (0, 1)^T, & \mathbf{b}_2 &= -\rho w^2 (1, 0)^T \end{aligned} \quad (A3)$$

Eq.16 is obtained by substituting Eq.A3 into Eq.A2.

Appendix B Derivation for Eq.27

The function U_I is given by

$$U_I = s\hat{V}_2/\mu \tag{B1}$$

where \hat{V}_2 is the Laplace transform of $V_2(y_1)$ defined by Eq.19 as

$$\hat{V}_2 = \int_0^\infty V_2\left(\frac{x_1 - \xi_1}{t}\right) e^{-st} dt = \mu(I_1 - I_2) \tag{B2}$$

where

$$I_1 = 4 \int_{t_2}^\infty \frac{t}{t_2} \sqrt{\left(\frac{t}{t_2}\right)^2 - 1} e^{-st} dt \tag{B3}$$

$$I_2 = \int_{t_1}^\infty \frac{t_2}{t} \frac{\left(2\left(\frac{t}{t_2}\right)^2 - 1\right)^2}{\sqrt{\left(\frac{t}{t_1}\right)^2 - 1}} e^{-st} dt \tag{B4}$$

and $t_i = |x_1 - \xi_1|/c_i, i = 1, 2$. The integrals I_1 and I_2 can be analytically integrated as

$$I_1 = 4 \frac{K_2(mst_1)}{s} \tag{B5}$$

$$I_2 = \frac{1}{s} \left[4K_2(st_1)/m^2 - 4(1 - 1/m^2)st_1K_1(st_1) + m^2st_1 \int_{st_1}^\infty K_0(\eta) d\eta \right] \tag{B6}$$

where K_n is the modified Bessel function of order n . Eq. 27 is obtained by first substituting Eq. B4 and Eq. B5 into Eq. B2 and the resulting expression is then substituted into Eq. B1.

Appendix C Derivation for Eq. 30, Eq. 35, and Eq. 36

The second term on the right side of (29) may be expressed in terms of [Erdogan, Gupta and Cook, 1974] as

$$\begin{aligned} & \int_{-1}^1 \frac{U_I(s|x_1 - (b_j + a_j\xi)|/c_1)}{b_j + a_j\xi - x_1} \frac{\hat{g}_j(\xi, s)}{\sqrt{1 - \xi^2}} d\xi \\ &= \frac{\pi}{N} \sum_{k=1}^N \frac{U_I(s|x_1 - (b_j + a_j\xi^{(k)})|/c_1)}{b_j + a_j\xi^{(k)} - x_1} \hat{g}_j(\xi^{(k)}, s) \end{aligned} \tag{C1}$$

where $\xi^{(k)}$ is given by Eq. 32. Eq. C1 is valid for arbitrary x_1 with $|x_1 - b_j| > a_j$ and $x_1 = b_j + a_j x^{(\ell)}$ for $|x_1 - b_j| < a_j$, where $x^{(\ell)}$ is given by Eq. 33.

To treat the first term on the right side of Eq.29 for $|\xi_1 - b_j| \leq a_j$, expand $\hat{g}_i(\xi, s)$ as

$$\hat{g}_i(\xi, s) = \sum_{m=0}^{N-1} d_m T_m(\xi) \tag{C2}$$

where d_m are constants and T_m is the m -th order Chebyshev polynomial of the first kind given by $T_m(\xi) = \cos(m \cos^{-1} \xi)$. From the orthogonality relations of the Chebyshev polynomials, the constants d_m can be expressed as

$$d_m = \frac{2}{N} \sum_{k=1}^{N_c} \hat{g}_i(\xi^{(k)}, s) \cos m\varphi^{(k)} \tag{C3}$$

Substitution of Eq. C3 into Eq. C2 yields

$$\hat{g}_i(\xi, s) = \frac{1}{N} \sum_{k=1}^N \left(1 + 2 \left(\sum_{m=1}^{N-1} \cos m\varphi^{(k)} T_m(\xi) \right) \right) \hat{g}_i(\xi^{(k)}, s) \tag{C4}$$

and

$$\int_x^1 \frac{\hat{g}_i(\xi, s)}{\sqrt{1-\xi^2}} d\xi = \frac{1}{N} \sum_{k=1}^N \left[\theta + 2 \left(\sum_{m=1}^{N-1} \frac{\cos m\varphi^{(k)} \sin(m\theta)}{m} \right) \right] \hat{g}_i(\xi^{(k)}, s) \tag{C5}$$

where $\theta = \cos^{-1} x$. From Eq. C5 and the crack closure conditions of Eq.25 lead to

$$\sum_{k=1}^N \hat{g}_i(\xi^{(k)}, s) = 0 \tag{C6}$$

and Eq. C5 is simplified as

$$\int_x^1 \frac{\hat{g}_i(\xi, s)}{\sqrt{1-\xi^2}} d\xi = \frac{2}{N} \sum_{k=1}^N \left(\sum_{m=1}^{N-1} \frac{\cos m\varphi^{(k)} \sin(m\theta)}{m} \right) \hat{g}_i(\xi^{(k)}, s) \tag{C7}$$

Eq. 30 is obtained by substituting Eq. C1 and Eq. C7 into Eq. 29 with $x_1 = b_i + a_i x^{(\ell)}$.

The stress intensity factors of the crack tips $x_1 = b_i \pm a_i$ can be calculated from the dislocation density as

$$\hat{K}_I(b_i \pm a_i, s) = \pm \frac{\mu}{1-\nu} \sqrt{\frac{\pi r}{2}} \lim_{r \rightarrow 0} \hat{\alpha}_2(r, s) \tag{C8}$$

where r is the distance from the crack tip. From Eq. 28, Eq. C8 can also be expressed as

$$\hat{K}_I(b_i \pm a_i, s) = \pm \frac{1}{2} \frac{\mu}{1-\nu} \sqrt{\frac{\pi}{a_i}} \hat{g}_i(\pm 1, s) \tag{C9}$$

From Eq. C4, Eq. C9 becomes

$$\hat{K}_I(b_i \pm a_i, s) = \pm \frac{\mu}{1-\nu} \frac{1}{N_C} \sqrt{\frac{\pi}{a_i}} \sum_{k=1}^{N_C} \left(\sum_{m=1}^{N_C-1} (\pm 1)^m \cos m\varphi^{(k)} \right) \hat{g}_i(\xi^{(k)}, s) \tag{C10}$$

where Eq. C6 is used. Eq. 35 and Eq. 36 are obtained from Eq. C10 with the following identities:

$$\sum_{m=1}^{N_C-1} \cos m\varphi^{(k)} = \frac{1}{2} \left[(-1)^{k+1} \cot \frac{\varphi^{(k)}}{2} - 1 \right]$$

$$\sum_{m=1}^{N_C-1} (-1)^m \cos m\varphi^{(k)} = -\frac{1}{2} \left[(-1)^{N_C} (-1)^{k+1} \tan \frac{\varphi^{(k)}}{2} + 1 \right]$$

and Eq.C6.